FRANZ LEBERL
Technical University
A-8010 Graz, Austria

Accuracy Analysis of Stereo Side-Looking Radar*

Radar stereo geometry and the accuracy of derived coordinates and coordinate differences are reviewed.

INTRODUCTION

STEREO SIDE-LOOKING RADAR (SLR) studies have so far been mainly academic exercises—few mapping applications have been found. This is different from mapping with single image SLR and SLR blocks, which did find extensive practical use.

Some geoscientists are, indeed, tempted to believe that the apex of SLR-imaging is past. The U.S. military topographic radar mapping program, for one, was terminated around 1972, and large cloud-covered remote areas of the world (though by far not all) have already been mapped. But imaging radar is very much alive. We find that research interests in SLR imaging are presently shifting from aircraft to satellite. We already have had the lunar Apollo-17-ALSE and Seasat-A projects, and many other satellite radar projects are being discussed or are in preparation, of which a rather spectacular one may be the Venus Orbital Imaging Radar (with the judicious acronym VOIR, which is French for "to see"). It is in the context of this development that stereo SLR analyses not only serve an academic interest but also may find an actual application in the planning of satellite SLR mapping efforts. The number of singular publications which have helped in the past to better understand the possibilities and limitations of stereo SLR are still very current. This paper is an account of that fact and presents an attempt at a review of the state-of-knowledge of stereo side-looking radar.

It is well established that stereo-viewing of SLR images can enhance the interpretation of morphological details (Koopmans, 1973), it can be used to measure slopes and relative height differences (Dalke and McCoy, 1969), and it can improve the accuracies of cartographic mapping and point positioning (Gracie *et al.*, 1970; DBA-Systems, 1974; Leberl, 1978).

ABSTRACT: *Renewed interest exists in stereo side-looking radar in the context of satellite projects to map the surface of the Earth and of Venus (Venus Orbital Imaging Radar, VOIR). This has led to the present review of known facts about stereoscopic vision with radar, of vertical exaggeration, of radar stereo geometry, and of the accuracy of radar derived coordinates and coordinate differences.*

Generally the term stereo refers to visual perception when an observer views an overlapping stereo image pair and in his brain forms a three-dimensional replica of the imaged area. But stereo may also be used for a computation process employing monocular measurements of homologue details in overlapping images.

Radar stereo is perceived in a manner similar to its photographic equivalent, although geometries are quite different as is demonstrated in Figure 1. Our understanding of visual SLR-stereo is largely due to the work of LaPrade (1963, 1970, 1975). Accuracy analyses were performed by several authors. Innes (1964), Rosenfield (1968), LaPrade (1970), Gracie *et al.* (1970), Konecny

* This paper is an abbreviated version of JPL Publication 79-17, *Accuracy Aspects of Stereo Side-Looking Radar*, March 1, 1979, Jet Propulsion Laboratory, Pasadena, California. The work was performed at JPL while the author was on leave from the Technical University, Graz.

PHOTOGRAMMETRIC ENGINEERING AND REMOTE SENSING,
Vol. 45, No. 8, August 1979, pp. 1083-1096.

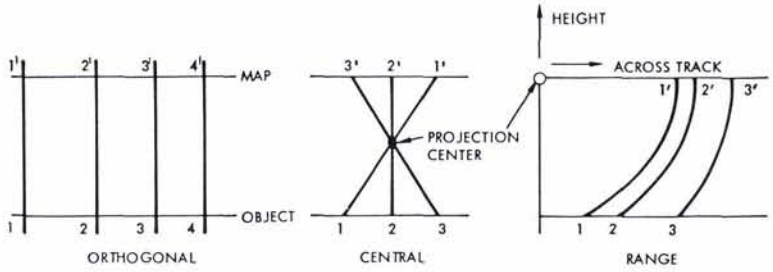

FIG. 1. Comparison of basic geometries for orthogonal, central, and range projection.

(1972), DBA-Systems (1974), Goodyear (1974), Derenyi (1975), Graham (1975, 1976), Leberl (1972, 1975, 1978), Carlson (1973), and Bair and Carlson (1974, 1975) all studied stereo SLR performance using various computational means.

In spite of this extensive list of studies, there are still many open stereo questions that need to be answered in the planning of SLR projects. The present paper, therefore, will not merely review the existing state-of-knowledge but will also try to fill in some areas, particularly where theoretical accuracy models for stereo SLR are concerned.

The paper will thus first address questions of visual stereo SLR and the geometry of the radar stereo model. A discussion of vertical exaggeration in aircraft and satellite radar follows. Then the errors of the stereo SLR model will be analyzed, both for coordinates and for measurement of distances and height differences. This analysis goes beyond a mere review and presents some original research.

VISUAL RADAR STEREO

STEREOSCOPY

Binocular vision of a pair of object points, A and P, leads to a situation that has been modeled by LaPrade *et al.* (1975) as illustrated by Figure 2. A convergence angle, γ, and retinal disparity angle, α, can be defined which lead to an observation of point A at a distance different from that of point P. Experimental work has shown that a human observer is sensitive to a minimal retinal disparity angle, α, of about 3^{cc} (LaPrade *et al.*, 1975) to 10^{cc} (Nowicki, 1966), and that an $\alpha > 1°$ may be difficult to view.

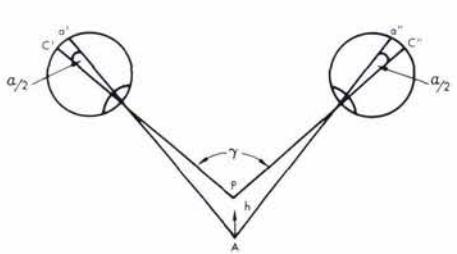

FIG. 2. Binocular vision and retinal disparity, α (from LaPrade *et al.*, 1975).

Stereoscopic viewing is a simulation of binocular vision by presenting to the eyes two overlapping images of an object. Today we understand stereoscopic viewing of camera photography largely due to the work of Aschenbrenner (1952), Fichter (1954), LaPrade (1972, 1973), LaPrade *et al.* (1975), and others.

It is a straightforward extension of camera stereo models that leads to an analysis of visual radar stereo. Figure 3 presents the most commonly discussed SLR flight configurations for stereo, the so-called same-side and opposite-side cases, obtained in two separate flights. They were proposed by LaPrade (1963). Other SLR stereo configurations are listed in Figure 4. Leberl (1972) and Graham (1975) proposed cross-wise flights; similarly, flights at different altitudes would be possible; and finally one could think of a range of convergent schemes, of which some have been discussed by Carlson (1973), Bair and Carlson (1974, 1975), and Leberl (1972).

Single flight line stereo cannot be realized with synthetic aperture radar (SAR). One may be tempted to believe that one can obtain two stereo looks by once imaging with a positive Doppler (looking forward or forward squint) and once with a negative Doppler (looking backwards or backward squint). But relief displacements would always be of the same amount and at an angle of 90° toward the nadir line, irrespective of the amount of Doppler frequency (or squint) used. As a result there will be zero parallax and no valid stereo (Leberl, 1972).

Figure 5 shows a SAR stereo configuration

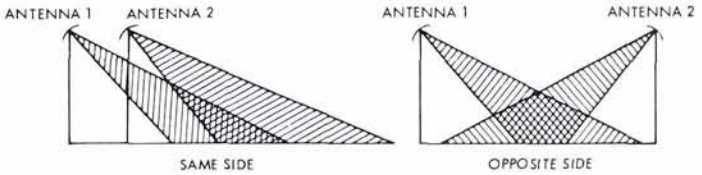

FIG. 3. Basic stereo radar configurations.

with forward and backward squint. The geometric locus of a point, *P*, would in each radar view be defined as a circle (intersection of (a) a sphere with radius equal to the slant range, i.e., a range sphere, and (b) a Doppler cone with a vertex angle defined by the Doppler frequency used). The two circles of the forward and backward view will coincide and, therefore, not produce a valid intersection.

Single flight stereo schemes could be effectively realized with real aperture radar by tilting the radar antennas around horizontal and/or vertical axes and using conical beams. In view of the future significance of SAR in satellites and of the importance of the basic same-side and opposite-side cases, we will pursue only these two cases in the remainder of the paper.

FACTORS AFFECTING VISUAL STEREO RADAR

In order to visually perceive a three-dimensional model of an object, the two images of a stereo pair must be sufficiently similar, i.e., image quality, object illumination, tones, and textures must be comparable and the retinal disparities caused by stereo parallaxes (geometric differences) must not exceed a value of about 1°. In aerial photography we find this rarely to present a

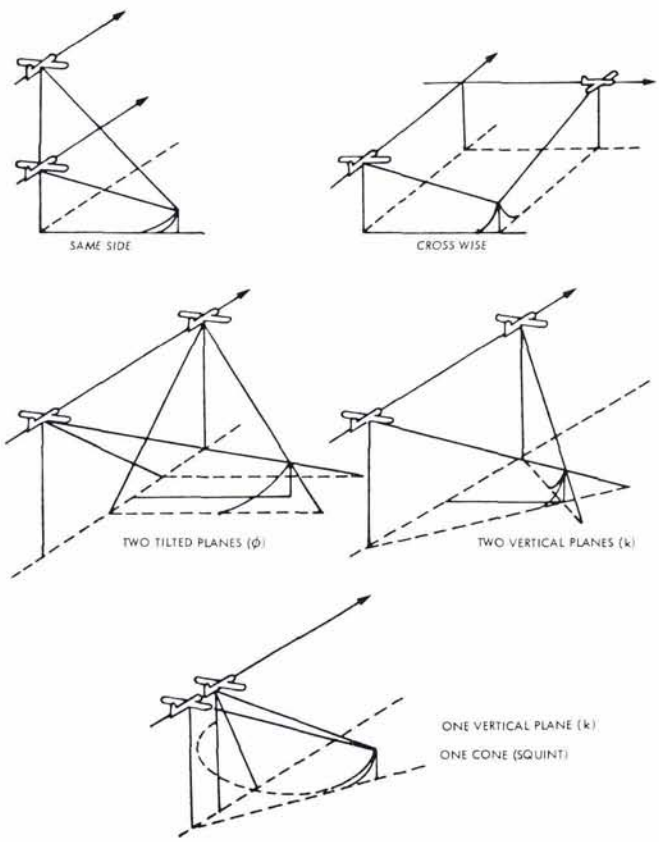

FIG. 4. Stereo configurations.

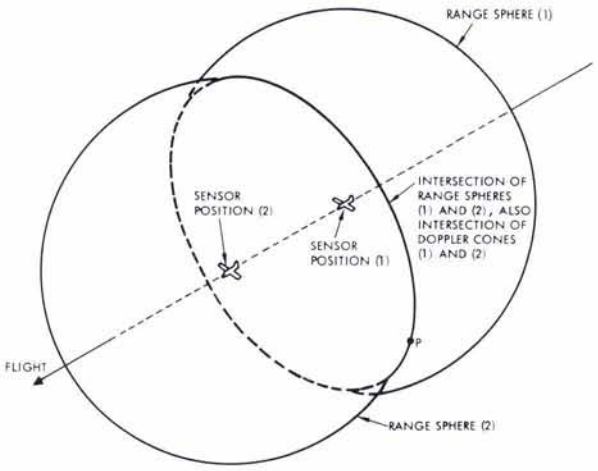

FIG. 5. Intersection of two projection lines in single flight "stereo" configuration with non-zero doppler processing not defined. Intersection lines of range sphere and doppler cone coincide.

problem: sun angles do not change drastically in overlapping photos. On the other hand, in the active radar system illumination depends on sensor position. Finally, parallaxes in aerial photography will be excessive only in the most extreme cases.

Figures 6 to 9 present examples of radar stereo pairs to demonstrate some of the limits to stereo viewing. Figure 6 shows part of the Estrella mountain in Arizona, imaged with an opposite-side configuration from an aircraft at 12 km altitude. It can be observed that slopes reflecting strongly in one image are in the radar shadow in the other image. A stereo impression cannot be achieved in the mountains but can in the flat areas. Figure 7 demonstrates with a same-side stereo pair that viewing does not present any problems. Koopmans (1973) was able to show that in some tropical areas of Colombia this type of same-side radar stereo produced a more complete drainage analysis than that from available (poor quality) aerial photography.

However, there also exist limits to successful same-side stereo. Figures 8 and 9 present two Apollo 17 lunar satellite stereo pairs with same-side geometry and stereo bases, b, of 3 and 13 km, respectively, and a flying height, H, of 116 km. Look angles are much steeper than in the previous examples ($\theta < 20°$); relief displacements and variations in image appearance are, thus, large even with a small stereo base. In the flat parts of Figure 8 stereo perception is easy. However, in the rugged parts stereo fusion becomes nearly impossible due to the differences of image content. In the rugged area of Figure 9 this is even more apparent.

In a mere qualitative way one must conclude that successful radar stereo viewing depends on

- The stereo arrangement,
- The look angles off-nadir,
- The stereo intersection angles, and
- The ruggedness of the terrain.

In flat or gently rolling areas stereo will hardly ever present a problem. In rugged terrain stereo is possible with same-side geometry and improves with shallower look-angles, θ. For good visual stereo perception one would prefer small stereo intersection angles. This results in image pairs with little difference in tone and texture, but also little difference in geometry. For good topographic expression (vertical exaggeration) one requires large intersection angles. We find ourselves in a trade-off between geometric accuracy and ease of perception without much experimental work available upon which to base decisions. LaPrade's (1975) results apply to stereo observation of man-made objects and seem to indicate optimum stereo viewing if look angles vary between 37° and 67° off-nadir, with intersection angles of about 12° to 15°.

GEOMETRY OF RADAR STEREO

RIGOROUS STEREO INTERSECTION

Rigorous radar stereo intersection algorithms were used by Rosenfield (1968), Gracie *et al.* (1970), DBA-Systems (1974), Leberl (1972, 1976), and Dowideit (1976).

The same algorithm can be used for sonar, which is an underwater analogy of radar (Clerici and Konecny, 1978). These formulations are based on a position vector, $\boldsymbol{p}$, for object point, P; on sensor position, $\boldsymbol{s}$; on attitude or velocity vector, $\dot{\boldsymbol{s}}$; and on squint angle and slant range vector, $\boldsymbol{r}$, with length, r, as defined in Figure 10 (vectors are represented by underlining in Figure 10).

The unknown vector $\boldsymbol{p}$ (with its three components p_1, p_2, and p_3) must be computed from the following four equations:

$$|\boldsymbol{p} - \boldsymbol{s}'| = r' \tag{1}$$

$$|\boldsymbol{p} - \boldsymbol{s}''| = r'' \tag{2}$$

$$\dot{\boldsymbol{s}}' \cdot (\boldsymbol{p} - \boldsymbol{s}') = \sin\tau |\dot{\boldsymbol{s}}'| \; |\boldsymbol{p} - \boldsymbol{s}'| \tag{3}$$

$$\dot{\boldsymbol{s}}'' \cdot (\boldsymbol{p} - \boldsymbol{s}'') = \sin\tau |\dot{\boldsymbol{s}}''| \; |\boldsymbol{p} - \boldsymbol{s}''| \tag{4}$$

Equations 1 and 2 present two range spheres with origin at the two antenna stations, $\boldsymbol{s}'$ and $\boldsymbol{s}''$, and of radius, r' and r'', respectively. Equations 3 and 4 are so called (Doppler) cones. In the event that the squint angle, τ, is zero, the cones degenerate to a plane. Each image defines as the locus of point, P, an intersection of the range sphere and the cone or plane. As a result, the locus is a circle. Stereo intersection consists of intersecting the two circles produced at antenna stations, $\boldsymbol{s}'$ and $\boldsymbol{s}''$.

PARALLAX EQUATIONS

When discussing parallax radargrammetry, we must differentiate between two cases: ground range presentation and slant range presentation. Figure 11 illustrates for a vertical object, AB, the difference between the two types of radar image presentations. In one case, projection circles are intersected with the datum plane while, in the other case, they are intersected with a plane through the antenna longitudinal axis. Rosenfield (1968) and others have formulated parallax equations for same-side and opposite-side stereo using ground range presentations.

An interesting and simplified radar stereo computation and analysis results if the radar projection circles are locally replaced by plane wave fronts as shown in Figures 12a and 12b. Expressions to convert observed parallax differences between two points into height differences were derived by Koopmans (1974), Derenyi (1975), and Leberl (1975), and others. The following equations summarize the relationships that exist between parallax and object height differences, and derive simply from Figure 12:

Ground range presentation:

$$\begin{aligned} p' &= h \cot\theta' \\ p'' &= h \cot\theta'' \\ \Delta p &= p'' \mp p' = h\,(\cot\theta'' \mp \cot\theta') \\ h &= \Delta p/(\cot\theta'' \mp \cot\theta') \end{aligned} \tag{6}$$

Slant range presentation:

$$\begin{aligned} p' &= h \cos\theta' \\ p'' &= h \cos\theta'' \\ \Delta p &= p'' \mp p' = h\,(\cos\theta'' \mp \cos\theta') \\ h &= \Delta p/(\cos\theta'' \mp \cos\theta') \end{aligned} \tag{7}$$

where h is object height difference; p' and p'' are relief displacements, and Δp is the parallax difference due to height, h. The minus sign applies to same-side geometry and plus sign to opposite-side geometry.

In both Equations 6 and 7 we find that height difference, h, not only depends on Δp but also on look angles, θ' and θ''. The same parallax difference, Δp, produces different h in various sections of the stereo model (compare LaPrade, 1963).

We are accustomed from photography to having constant absolute parallax, i.e., no parallax differences, for points at equal height. This applies also to ground range presentation where all points in the datum plane have the same absolute parallax, a, i.e.,

$$a = y'' - y'$$

where y' and y'' are ground distances. This does not apply to slant range images.

Figure 13 is the example of a slant range radar image of an Atlantic island: it appears as though the island were rolled onto a cylinder. This visual impression is caused by the scale compression that increases towards the nadir line, as explained in Figure 14. We now define absolute parallax, a, as the difference of slant ranges, i.e.,

$$a = r' - r'' = (H^2 + y^2)^{1/2} - (H^2 - (y - B)^2)^{1/2} \tag{8}$$

where H is the flying height, y is the ground distance of an object from flight line ($'$), and B is the stereo base or distance between the two flight lines ($'$) and ($''$). One can easily verify that Equation 8 defines a curve similar to a hyperbola, so that the stereo model of a flat, horizontal surface represents a super-hyperbolic cylinder (Leberl, 1978). Equation 7 describes the height, h, of an object above this cylinder.

VERTICAL EXAGGERATION

A factor of considerable interest to image interpreters is the vertical exaggeration in radar stereo models. LaPrade (1970) and Graham (1976) have found quantitative

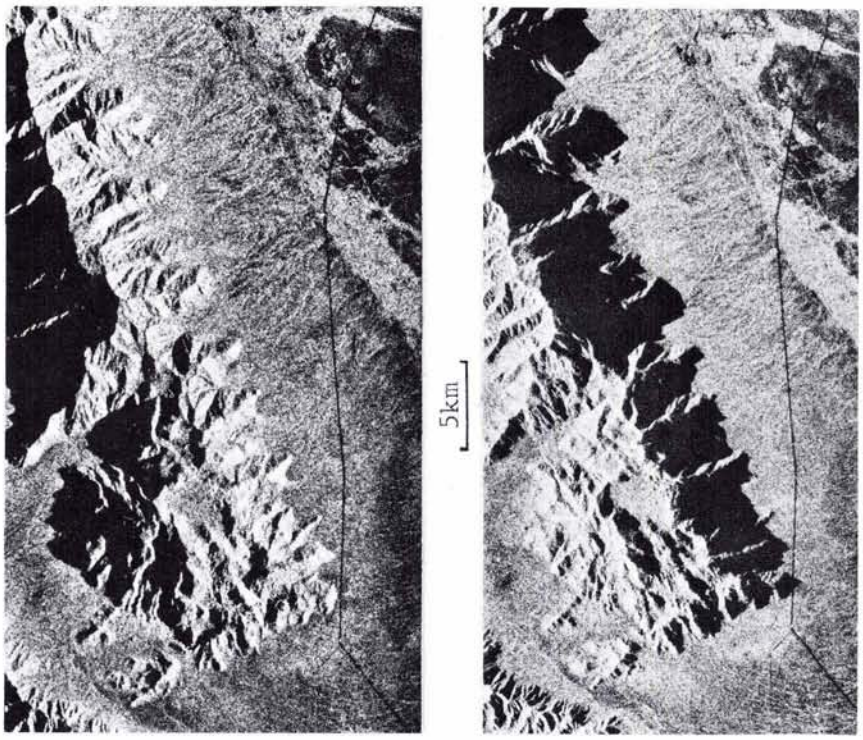

FIG. 6. Aircraft stereo radar, opposite-side geometry. x-Band, 12 km Altitude; Estrella Mountains, Arizona. (Courtesy of Aero Service, Goodyear).

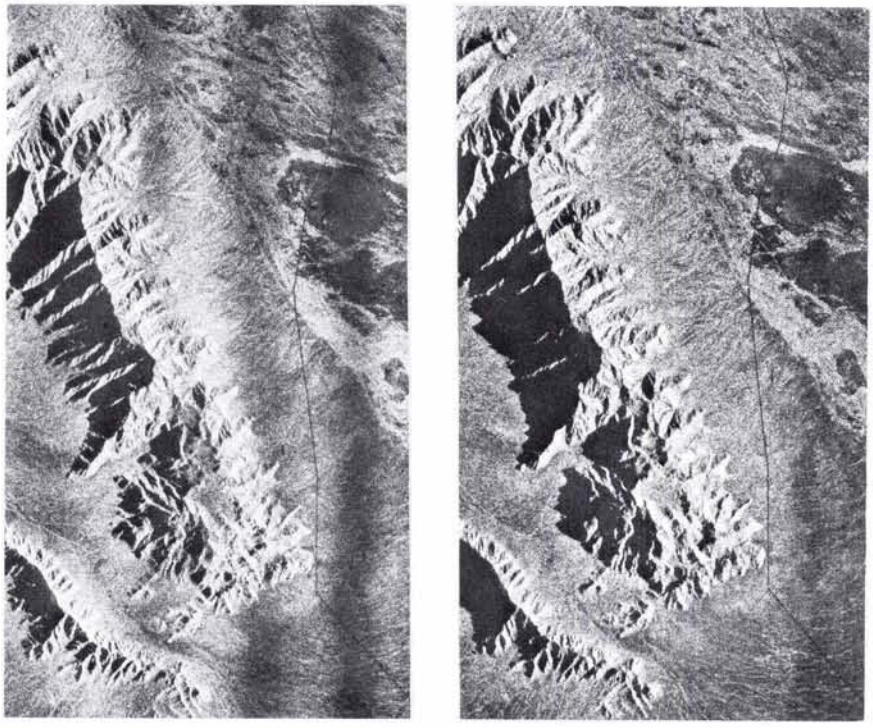

FIG. 7. Aircraft stereo radar, same-side geometry, otherwise the same as Figure 6.

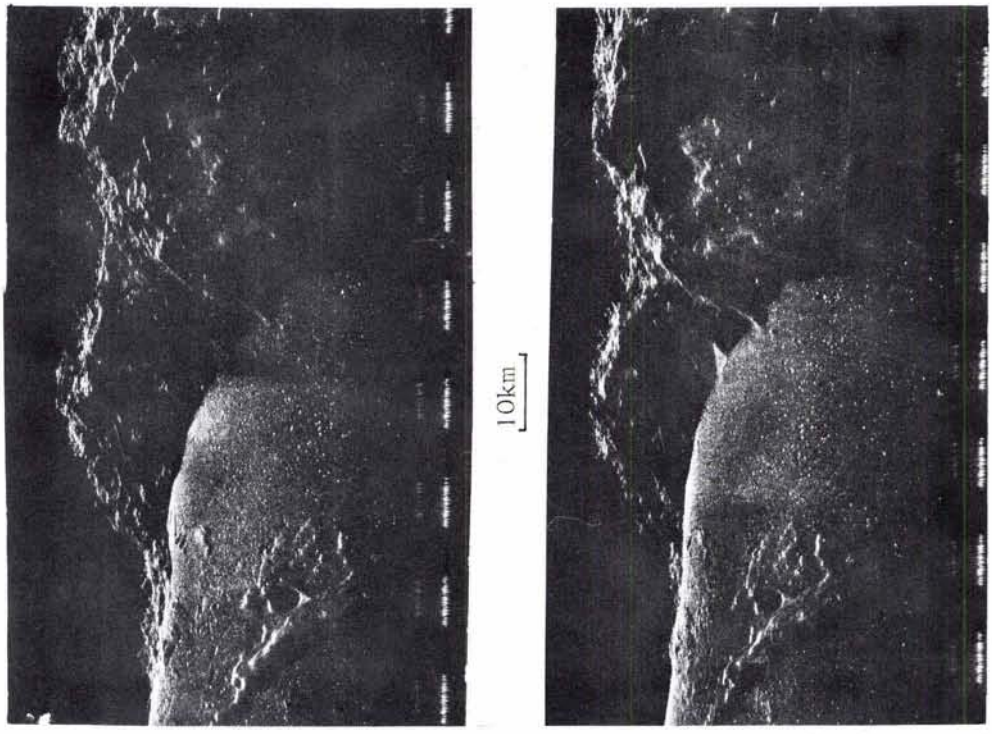

FIG. 8. Satellite stereo radar, same-side geometry. Apollo 17-Alse-VHF (2 m Wavelength), Appennin on the Moon (courtesy NASA-JPL). Stereo base ~3 km.

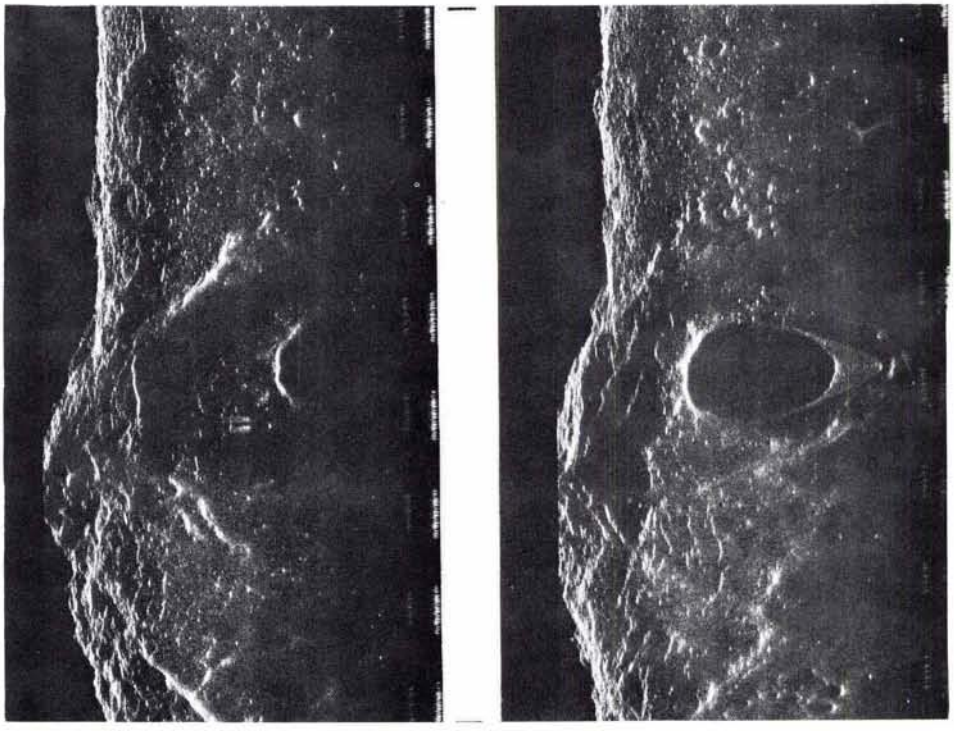

FIG. 9. Satellite stereo radar, same-side geometry as in Figure 8, but of the Oriental Region, on the lunar far side. Stereo base ~13 km.

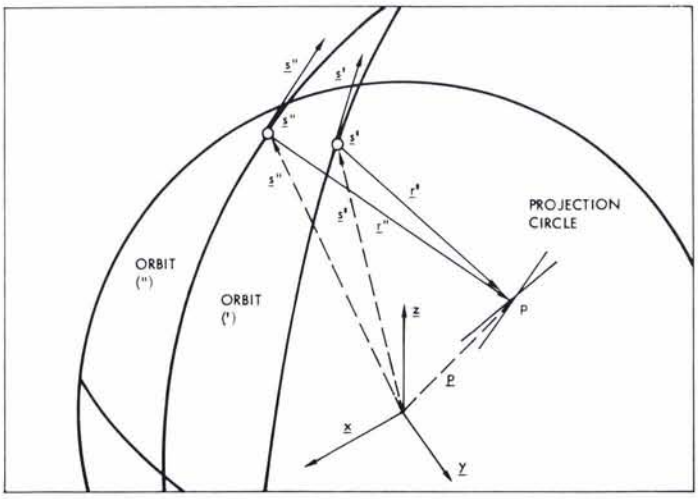

FIG. 10. Rigorous stereo intersection.

measures for this exaggeration by relating radar stereo parallax to the base-to-height ratio, B_e/H, of equivalent camera photography (compare Figure 12a). Equivalent photography is defined here in such a way that it produces the same parallax, Δp, from the same altitude, H. Clearly, the stereo base, B_e, is smaller than that of the radar.

The vertical exaggeration, q, is the ratio between the true height-to-base ratio, h/b, of an object and its virtually perceived stereo model equivalent, h_i/b_i. Following LaPrade (1972), factor q for photography as observed under a stereoscope usually is

$$q \approx 5 \cdot B_e/H. \tag{9}$$

We now need only to replace B_e/H by an equivalent radar expression. Since we know from photography that

$$B_e/H = \Delta p/h$$

and from ground range radar that

$$\Delta p/h = \cot \theta' \mp \cot \theta'',$$

we find

$$q \approx 5 \, (\cot \theta' \mp \cot \theta'') \tag{10}$$

or, with the notation of Figure 12 a,

$$q \approx 5HB/(y(y-B)). \tag{11}$$

Equation 11 was derived originally by Graham (1976).

For airborne radar, with 60 percent overlap and stereo intersection angles, $\Delta\theta$,

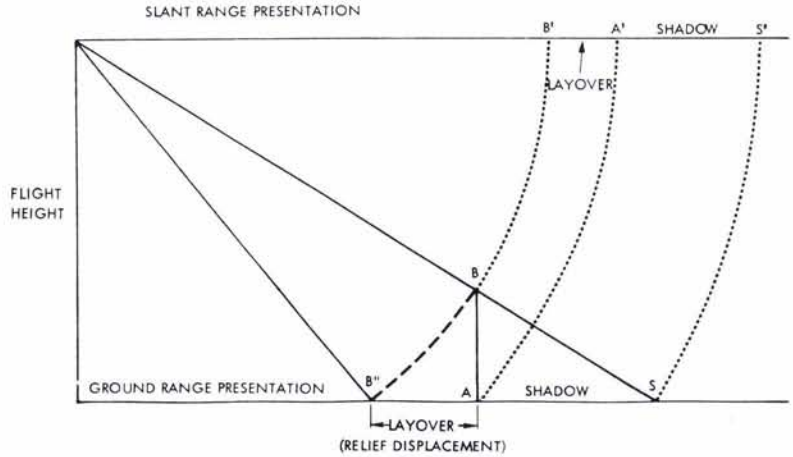

FIG. 11. Vertical object, definition of slant range and ground range presentations.

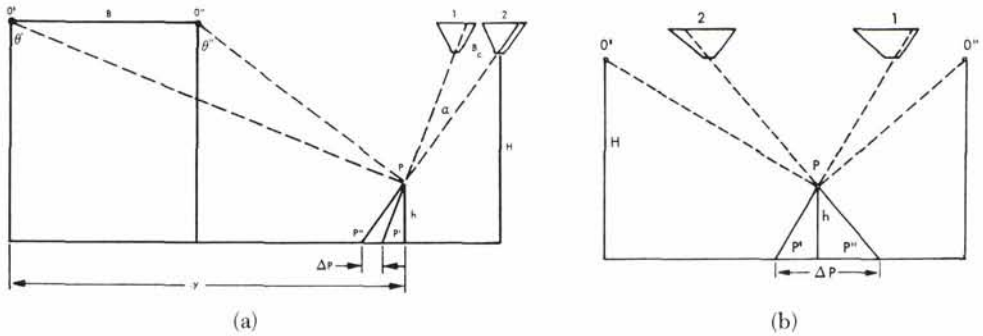

FIG. 12. Definition of radar stereo parallax, Δp, and relief displacement, p, for (a) same-side and (b) opposite-side stereo. Note the approximation of the spherical wavefront by a straight line. Also, note the equivalent camera arrangement to obtain the same stereo-parallax. (See also La Prade, 1970).

between 12° and 15°, one finds q ranging from 2.3 to 1.8. For a satellite radar such as the proposed VOIR (Venus mission), intersection angles, $\Delta\theta$, are poor, i.e., between 3°.3 and 2°.8, so that $q \approx 0.6$. These exaggeration factors are much smaller than those of aerial photography ($q \approx 3$).

ERRORS OF THE RADAR STEREO MODEL

In the following analysis of errors of the radar stereo model we differentiate between errors of individual point coordinates (absolute errors) and errors of coordinate differences (sometimes called relative errors).

Absolute error analyses have been published for airborne radar by Rosenfield (1968), LaPrade (1970), and Leberl (1972), and for satellite radar by Leberl (1978). Relative error studies, although of at least equal interest to those of absolute errors, have not come to the attention of the author.

ERRORS OF COORDINATES

Error sources are numerous, but most important are those caused by erroneous sensor positions $d\boldsymbol{s}' = (dx'_0, dy'_0, dz'_0)$ and $d\boldsymbol{s}'' = (dx''_0, dy''_0, dz''_0)$; by erroneous sensor attitudes $d\dot{\boldsymbol{s}}' = (d\dot{y}'_0, d\dot{y}'_0, d\dot{z}'_0)$ and $d\dot{\boldsymbol{s}}'' = (d\dot{x}''_0, d\dot{y}''_0, d\dot{z}''_0)$; and by erroneous slant ranges dr' and dr''.

The detailed derivation of coordinate errors due to each individual error source

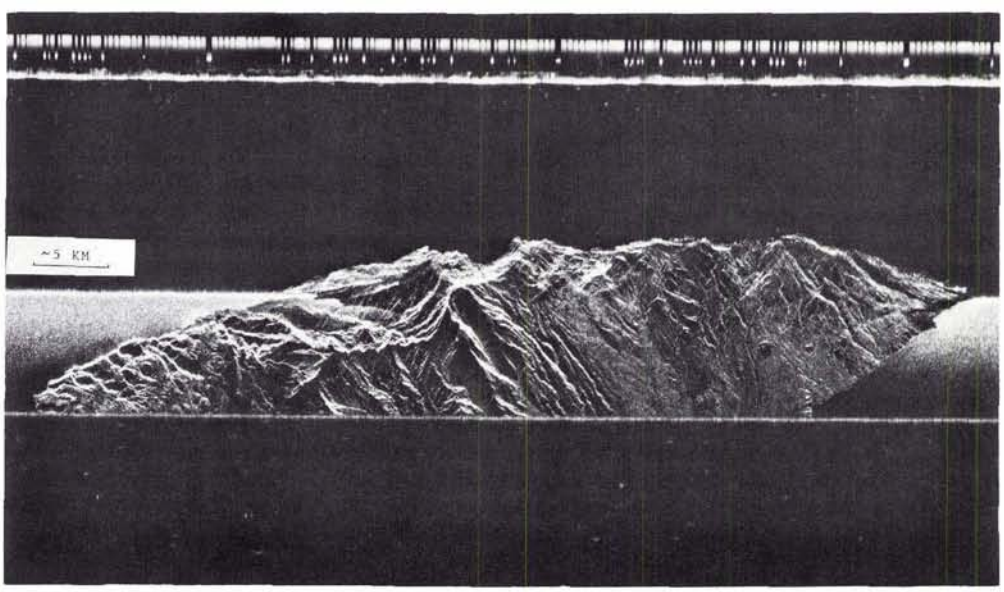

FIG. 13. Slant range radar image of an Atlantic island (courtesy NASA-JPL). Image taken from 10 km flight altitude.

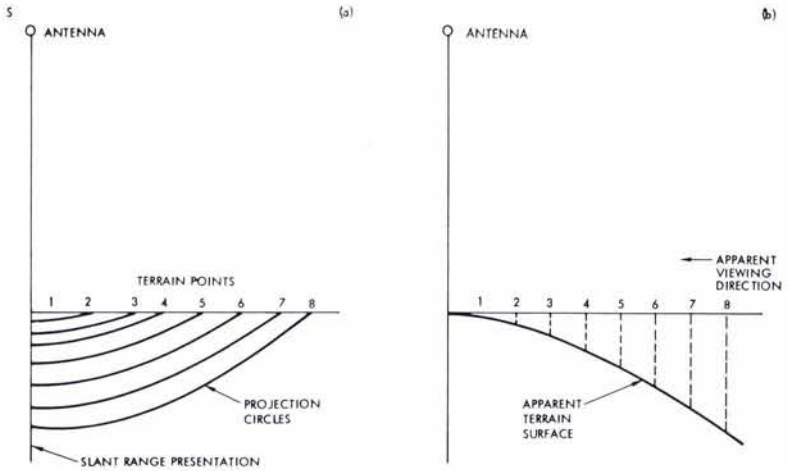

FIG. 14. Visual impression obtained from slant range presentation.

would go beyond the scope of this paper. Instead, the errors of x,y,z coordinates are derived due to only one error source, i.e., sensor position error dy''_0. All others are just listed in one formula, with reference to a detailed derivation in Leberl (1979).

Considering Figure 15, we find that the presence of an error, dy''_0, shifts the intersection of two wavefronts from point (P) to point P. As a result we have coordinate errors dy and dz, while $dx = 0$.

Since

$$dy = l \cos \theta' = l \cdot H/r'$$

and

$$l = dy''_0 \sin \theta''/\sin (\theta' - \theta''),$$

one finds that

$$dy = H\, dy''_0 \sin \theta''/(r' \sin (\theta' - \theta''))$$

or, due to

$$r'/B = \sin (90^\circ + \theta'')/\sin (\theta' - \theta''),$$

we get

$$\begin{aligned} dy &= -dy''_0 \cdot H \cdot \tan \theta''/B \\ &= dy''_0 (B-y)/B. \end{aligned} \tag{12}$$

Similarly, we can derive coordinate changes due to other changes of imaging parameters. One then gets the following long expressions:

$$\begin{aligned} dx = {} & (dx'_0 + dx''_0)/2 + d\dot{y}'_0 \cdot y/2 + d\dot{y}''(y-B)/2 \\ & + (d\dot{z}'_0 + d\dot{z}''_0) \cdot H/2 \end{aligned} \tag{13}$$

$$\begin{aligned} dy = {} & dy'_0 \cdot y/B + dy''_0(B-y)/B - (dz'_0 - dz''_0)H/B \\ & + dr' \cdot r'/B - dr'' \cdot r''/B \end{aligned} \tag{14}$$

$$\begin{aligned} dz = {} & (dy'_0 - dy''_0)y \cdot (y-B)/(H \cdot B) - dz'_0(y-B)/B \\ & + dz''_0 \cdot y/B + dr' \cdot r' \cdot (y-B)/(BH) \\ & - dr'' \cdot r'' \cdot y/(BH) \end{aligned} \tag{15}$$

An evaluation of these equations confirms the findings of Rosenfield (1968) and others. Figure 16 illustrates two typical configurations, one for aircraft and the other for a proposed VOIR-satellite. We find in the near range area of the aircraft stereo model that error coefficients are all about 1, with dz being smaller than dy. In the far range area, the error coefficients grow to about 2 to 5, but now with dy smaller than dz.

In a satellite radar for VOIR the error coefficients are about 10 times larger than those for aircraft. Again, at the near range edge of the stereo model dy is greater than dz, and the reverse applies at far ranges.

ERRORS OF COORDINATE DIFFERENCES

Radar stereo can essentially be a means of interpolating coordinates in between known points. Therefore, it is the error of coordinate differences that counts in the evaluation of radar mission alternatives. In this context it is legitimate to study errors due to only three error sources, i.e., those due to an error, dB, in the stereo base, B; an erroneous height difference, dH, between corresponding antenna positions; and errors dr' and dr'' in slant range. The along-track model coordinate, x, is not affected by these errors; therefore, we need only consider model coordinates y and z.

Error of the Stereo Base: dB. We introduce the notation $dB = dy''_0 - dy'_0$ and find from the first two terms of Equations 14 and 15 that

$$dy = -\frac{y}{B} dB + \text{const} \tag{16}$$

$$dz = \{(B-y)y/(BH)\}\ dB \tag{17}$$

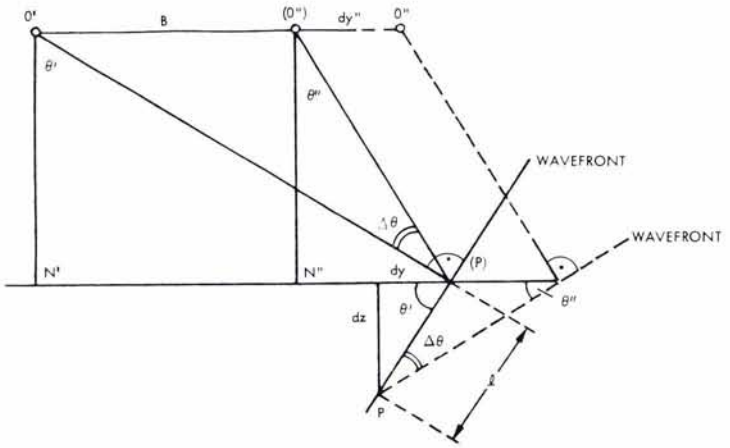

FIG. 15. Errors due to the y''_0—component of sensor position.

The errors of coordinate differences are found by partial differentiation of these equations with respect to y and z. This is done in order to get the changes, $d\Delta y$ and $d\Delta z$, of coordinate errors, dy and dz, as a function of the coordinate changes, Δy and Δz, i.e.,

$$d\Delta y = (-\Delta y/B) \cdot dB \tag{18}$$

$$d\Delta z = \{\Delta y \cdot (B-2y)/(BH) - \Delta z(y \cdot (B-y)/(BH^2)\} \, dB \tag{19}$$

Equations 18 and 19 are valid for small coordinate differences, Δy and Δz, in model space. Several conclusions can be drawn:

- cross track distances, Δy, have errors directly proportional to base errors, dB;
- height differences, Δz, have errors, $d\Delta z$, that are more complex, i.e., for vertical structures ($\Delta y = 0$) errors increase as a 2^{nd} order function of y; and
- height differences, Δz, measured between two points at distance, Δy, have an error that changes linearly with y.

Error of Flight Height: dH. We introduce the notation $dH = dz''_0 - dz'_0$ and find from Equations 14 and 15 that

$$dy = \frac{H}{B} dH \tag{20}$$

$$dz = \frac{y}{B} dH + \text{const} \tag{21}$$

By partial differentiation with respect to y and z, we obtain the simple proportionality

$$d\Delta y = \frac{dH}{B} \Delta z \tag{22}$$

$$d\Delta z = \frac{dH}{B} \Delta y \tag{23}$$

Errors of Slant Ranges: dr' and dr". Errors in the slant range may be systematic, for example due to scaling errors, and random, due to limited range resolution. Systematic errors lead to a model bow, and random errors to a limited height definition. Similarly, the y-coordinate is subject to a limited definition.

The systematic model warp due to errors, dr' and dr'', follows the equations

$$\begin{aligned} d\Delta y &= A\ \Delta y + F\ \Delta z \\ d\Delta z &= C\ \Delta y + D\ \Delta z \end{aligned} \tag{24}$$

where

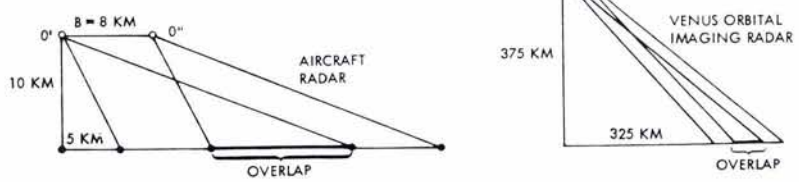

FIG. 16. Stereo configurations for numerical analysis.

TABLE 1. STEREO MODEL ERRORS IN METRES. dy AND dz ARE ERRORS IN COORDINATES, y AND z. $d\Delta y$ AND $d\Delta z$ ARE ERRORS OF COORDINATE DIFFERENCES, Δy AND Δz. FLIGHT CONFIGURATIONS ARE AS IN FIGURE 16. ERRORS ARE LISTED FOR EACH INDIVIDUAL ERROR SOURCE dB, dH, dr'', dy_0'', dz_0''.

	AIRCRAFT (B = 8km, H = 10km)						VOIR (B = 40km, H = 375km)					
	Near Range y = 13km			Far Range y = 25km			Near Range y = 365km			Far Range y = 425km		
	dy_0'' 100m	dz_0'' 10m	dr'' 10m	dy_0'' 100m	dz_0'' 10m	dr'' 10m	dy_0'' 1km	dz_0'' 100m	dr'' 100m	dy_0'' 1km	dz_0'' 100m	dr'' 100m
dy	−63	12.5	−20.5	−213	12.5	−24.7	−8130	938	−1240	−9630	938	−1344
dz	81	16.3	−26.7	531	31.3	−61.6	−7910	813	−1075	−10910	1063	−1523
	dB 100m	dH 10m	dr'' 10m	dB 100m	dH 10m	dr'' 10m	dB 1km	dH 100m	dr'' 100m	dB 1km	dH 100m	dr'' 100m
$d\Delta y$ $\Delta y = 0, \Delta z = 1$	0	1.2	−0.4	0	1.2	−0.2	0	2.5	0	0	2.5	0
$d\Delta y$ $\Delta y = 1, \Delta z = 1$	−12.5	1.2	0	−12.5	1.2	0	−25	2.5	0	−2.5	2.5	0
$d\Delta z$ $\Delta y = 0, \Delta z = 1$	8.1	0	−0.3	53.1	0	−0.3	21	0	0	+29	0	0
$d\Delta z$ $\Delta y = 1, \Delta z = 1$	−14.4	1.2	0.1	0.6	1.2	−0.2	−25	2.5	0	−25	2.5	0

$$A = dr'y/(Br') - dr''(y-B)/(Br'')$$
$$F = dr'H/(Br') - dr'' H/(Br'')$$
$$C = dr'(r'/(B \cdot H)+y(y-B)/(BHr')) - dr''(r''/(BH)+y(y-B)/(B \cdot H \cdot r''))$$
$$D = dr'((y-B)/(Br')-(y-B)r'/(BH^2)) - dr''(y/(Br'')-yr''/(BH^2))$$

The limited definitions of y and z due to random noise in the slant range, σ_r^2, are σ_y^2 and σ_z^2, i.e.,

$$\sigma_y^2 = \sigma_r^2(r'^2 + r''^2)/B^2 \qquad (25)$$
$$\sigma_z^2 = \sigma_r^2(r'^2(y-B)^2 + r''^2y^2)/(B^2H^2)$$

Discussion. From the expressions derived here we find that errors in (small) distances and height differences are different from errors in coordinates. Table 1 illustrates some figures for aircraft or VOIR radar configurations as in Figure 16.

An example illustrates the errors that can occur:

Error dB = 100 m
Center of stereo model,
$\Delta z = \Delta y$ = 1 km

Aircraft	VOIR
dz = 261 m	dz = 935 m
dy = 237 m	dy = 988 m
$d\Delta z$ = −11 m	$d\Delta z$ = −2.5 m

The limited resolution of slant range creates random errors of model height and cross-track coordinates. For the VOIR and a σ_r = ±100 m, this is $\sigma_z = \sigma_y \approx \pm 1{,}9$ km.

Conclusion

Basic facts regarding stereo side-looking radar were reviewed and illustrated both for aircraft and for spacecraft radar configurations. Both visual stereo geometry and stereo model accuracy were evaluated, and numerous formulas were reviewed or derived in order to provide a basis for discussion and quantitative judgment. In this way the concept of vertical exaggeration serves to evaluate the quality of radar stereo. Two examples are presented: optimum aircraft stereo offers an exaggeration factor, q, of about 2 and a Venus Orbital Imaging Radar (VOIR) with an exaggeration factor of only 0.6.

In the discussion of stereo model accuracies one differentiates between errors of coordinates (absolute accuracy) and of distances and height differences (relative errors). These errors have different magnitudes. It is also shown that these (relative) errors of coordinate differences are much less sensitive to an erroneous stereo base or flight height than is the case with errors in the coordinates themselves.

A number of factors have an effect on the ability to actually observe a radar stereo model, e.g., look angles, terrain types, stereo intersection, and configurations. There exist some indications that look angles should be not less than 40° off-nadir, with intersection angles of about 15°. However, this area needs further study, mainly of an experimental nature.

Acknowledgment

I am grateful for the support received during this study at the Jet Propulsion Laboratory, in particular from Dr. C. Elachi. I would like to thank also Mr. G. LaPrade and Mr. L. Graham, both of Goodyear Aerospace Corp., for their advice and help.

References

Aschenbrenner, C. M., 1952. A Review of Facts and Terms Concerning the Stereoscopic Effect, *Photogrammetric Eng.*, Vol. 18.

Bair, G. L., and G. E. Carlson, 1974. Performance Comparison of Techniques for Obtaining Stereo Radar Images, *IEEE Trans. on Geoscience Electronics*, Ge-12.

————, 1975. Height Measurement with Stereo Radar, *Photogrammetric Eng. and Remote Sensing*, Vol. 41, No. 2, pp. 167-176.

Carlson, G. E., 1973. An Improved Single Flight Technique for Radar Stereo, *IEEE Trans. on Geoscience Electronics*, GE-11, No. 4., pp. 199-204.

Clerici, E., and G. Konecny, 1978. A Study in the Determination of Depth Information from Underwater Acoustical Scanners, Symposium of Comm. III, Int. Soc. of Photogrammetry, Moscow, USSR, 31 July—5 August 1978. Published in: *Nachrichten aus dem Karten-und Vermessungswesen*, Reihe II, 36, Inst. for Applied Geodesy, Frankfurt a.M., Germany.

Dalke, G., and M. McCoy, 1969. Regional Slopes with Non-Stereo Radar, *Photogrammetric Engineering*, Vol. 35, No. 5, pp. 446-452.

DBA-Systems, 1974. *Research Studies and Investigations for Radar Control Extensions*, DBA Systems, Inc., P.O. Drawer 550, Melbourne, Florida, Defense Documentation Center Report No. 530784L.

Derenyi, E. E., 1975. Topographic Accuracy of Side Looking Radar Imagery, *Bildmessung und Luftbildwesen*, 1975, No. 1.

Fichter, A. J., 1954. Geometry of the Imaginary Stereo Model, *Photogrammetria*, Vol. 10, pp. 134-139.

Goodyear, 1974. *Preliminary Imagery Data Analysis Goodyear Electronic Mapping System (GEMS)*, Goodyear Aerospace Corp., Report GIB-9342, Code 99696.

Graham, L., 1975. Flight Planning for Stereo Radar Mapping, *Proc. Am. Soc. Photogramm.*, 41st Meeting, Washington, D.C.

_____, 1976. *Earth Resources Radar Stereo Considerations*, Goodyear Aerospace Corp., Arizona Div., AEEM-550, 13 p.

Gracie, G., *et al.*, 1970. *Stereo Radar Analysis*, U.S. Engineer. Topographic Laboratory, Ft. Belvoir, Virginia. Report No. FTR-1339-1.

Innes, R. B., 1964. *Principles of SLAR Measurement of the Third Coordinate of Target Position*, Report of Project Michigan No. 2900-474-T.

Konecny, G., 1972. Geometrical Aspects of Remote Sensing, *Arch. Int. Soc. Photogramm.*, Invited Paper, 12th Congress, Ottawa, Canada.

Koopmans, B., 1973. Drainage Analysis on Radar Images, *ITC-Journal*, 1973-3, Enschede, Netherlands.

LaPrade, G., 1963. An Analytical and Experimental Study of Stereo for Radar, *Photogrammetric Engineering*, Vol. 29, No. 2, pp. 294-300.

_____, 1970. *Subjective Considerations for Stereo Radar*, Goodyear Aerospace Corp., GiB 9169.

_____, 1972. Stereoscopy—A More General Theory, *Photogrammetric Engineering*, Vol. 38, pp. 1177-1187.

_____, 1973a. Stereoscopy—Will Facts or Dogma Prevail?, *Photogrammetric Engineering*, Vol. 39, pp. 1271-1275.

_____, 1973b. *A More General Theory of Stereoscopy*, Goodyear Aerospace Corp., Arizona Div., GiB-9268, Rev. A, 58 p.

_____, 1975. Addendum to GiB-9169, *Subjective Considerations for Stereo Radar*, Goodyear Aerospace Corp., Arizona Division.

LaPrade, G., *et al.*, 1975. *Stereoscopy*, Goodyear Aerospace Corp., Arizona Div., GERA-2120, Code 99696; 57 p.

Leberl, F., 1972. On Model Formation with Remote Sensing Imagery, *Österr. Zeitschrift für Vermessungswesen*, Vol. 60, pp. 93-61.

_____, 1975. *Radargrammetry for Image Interpreters*, ITC Techn. Report No. 2, Enschede.

_____, 1976a. Mapping of Lunar Surface from Side-Looking Orbital Radar Images, *The Moon*, Vol. 15, No. 3/4.

_____, 1976b. Imaging Radar Applications to Mapping and Charting, *Photogrammetria*, Vol. 32.

_____, 1978. *Satellitenradargrammetrie*, Deutsche Geodaetische Kommission, Series C, Nr. 239, Munich, 156 p.

_____, 1979. *Accuracy Aspects of Stereo Side-Looking Radar*, JPL Publication 79-17, Jet Propulsion Laboratory, Pasadena, California.

Nowicki, A. L., 1966. "Stereoscopy", Chapter 11 of *Manual of Photogrammetry*, 3rd edition, American Soc. of Photogrammetry, Falls Church, Va., USA.

Rosenfield, G. H., 1968. Stereo Radar Techniques, *Photogrammetric Engineering*, Vol. 34, No. 6, pp. 586-594.

(Received and accepted May 21, 1979)

BOOK REVIEW

Recognition of Tree Species on Aerial Photographs, by Leo Sayn-Wittgenstein. Forest Management Institute, Information Report FMR-X-118. Canadian Forestry Service, Department of the Environment. 97 p., 72 illus. November, 1978.

THIS IS A MANUAL designed to help photo interpreters recognize the most important Canadian tree species. Scale of photography, focal length, flying height, films and filters as well as ecological species characteristics and the pattern of species associations are discussed in general terms. Considerable emphasis is placed on the characteristic crown shapes and branching habits of individual trees and on seasonal variations as an aid to photo interpretation. The identifying characteristics of approximately 40 tree species are described in detail, with guidelines and keys for their identification. Many illustrations, in particular stereograms at large and medium scales, are included. Many are in color.

This publication is well referenced (39 citations) and has an appendix which includes phenological data on tree leafing and fall coloration in three areas of Canada. While few non-boreal species are included, the techniques described would guide an interpreter in developing his own recognition keys and stereograms.

The writing is good, and typographic errors are minimal. The publisher used hard clay-coated paper (8½ × 11 inches) and spiral-binding to facilitate stereo viewing.

—Robert C. Heller
University of Idaho